Resonance Properties of a LiPo Battery as a Proximity Coupled S Band Patch Antenna

Jason Wood, *Student Member, IEEE*

***Abstract*—A 24x18mm lithium polymer (LiPo) battery was resonated as a proximity coupled patch antenna equivalent for S band frequencies. Impedance matching was achieved using the standing wave on an open circuit microstrip feed line. The battery was oriented perpendicular to the feed line, with and without connecting the battery anode to ground. Return losses of -40dB and lower were consistently achieved, with average bandwidths of 1.76% to 3.53%. The LiPo battery could be efficiently resonated as a patch antenna equivalent, although measurements of the resultant antenna pattern are still required to determine its suitability as a functional antenna.**

***Index Terms*—Lithium Polymer, Patch Antenna, Proximity Coupled, S band**

I. Introduction

Microstrip patch antennas (MPA) are a versatile antenna used in many different applications requiring planar antennas. In portable electronics, their ease of fabrication (hence low cost), low weight, and relatively small size make them popular choices for high frequency communications. However, their narrow bandwidth and leakage radiation are the main disadvantages in mobile communications [1]. Previous research has focused largely on addressing these shortcomings through the use of different patch designs [2] and feed techniques [3, 4].

Proximity coupling is a non-contact feeding technique that could be used to drive a pre-existing component as a patch antenna equivalent. This could save PCB space in size limited applications by negating the need for a dedicated antenna, or provide supplementary UHF channels in addition to existing antennae (e.g. for RFID scanning). Although each channel would have a narrow bandwidth, multiple frequencies could be used with a single patch equivalent.

Lithium polymer (LiPo) batteries are ubiquitous in modern electronics, and contain conductive polymers which have been found to perform reasonably well as patch antenna materials [5]. The physical size of these batteries in handheld electronics also makes them suitable for resonating at UHF frequencies.

This paper was submitted for review in the IEEE Australia Student Paper Competition on Dec 30 2015.

J. Wood is with the School of Engineering, Griffith University, Nathan, QLD, Australia. Email jason.wood2@griffithuni.edu.au

II. Theory

A. Return Loss and Bandwidth

For a single port antenna, the voltage scattering parameter S_{11} is equal to the reflection coefficient Γ, of the antenna. This is used to define the power return loss (*RL*) as [6]:

$$RL = -20\log_{10}|\Gamma| \quad (1)$$

RL is a minimum at resonance, and was the main parameter investigated in this experiment.

A standard cutoff value for the RL is -10dB, above which an antenna is deemed to be inadequately matched to its feed line. The range of frequencies for which the RL is below this threshold is the impedance bandwidth. This may be different from the pattern bandwidth [7], which was not measured in this investigation.

B. Rectangular Patch Antenna Design

The length and width of a rectangular MPA, as well as the substrate it is mounted on, determines its operating characteristics. To resonate in the fundamental TM_{10} mode, with effective wavelength λ_{eff}, the patch length *L* should be $0.49\lambda_{eff}$. This is slightly less than half an effective wavelength, to account for the electromagnetic lengthening of the patch due to fringing fields. The effective wavelength is the free space wavelength divided by the square root of the effective permittivity [7]. Higher order modes will also resonate when the patch length is an odd multiple of $0.5\lambda_{eff}$. This can occur for both the length and width of a patch antenna, which creates cross-polarisation. To avoid this, the patch must be fed at the centre of its width, so that fields along its width cancel out [1].

While the length of a patch determines its resonance, the width *W* and substrate properties (height *h* and relative permittivity ε_r) determine the bandwidth, edge input impedance and radiating efficiency [1]. For a patch antenna with known dimensions, its fundamental resonant frequency can be determined as follows.

Firstly, the effective relative permittivity differs from that of the substrate, since fringing fields exist both in the substrate and the medium above the antenna. For $W/h \geq 1$, the following approximation can be made for $\varepsilon_{r_{eff}}$ [1]:

$$\varepsilon_{r_{eff}} = \frac{\varepsilon_r + 1}{2} + \frac{\varepsilon_r - 1}{2}\left(1 + \frac{12h}{W}\right)^{-1/2} \quad (2)$$

This can then be used to determine the effective length of the patch, which is the sum of its physical length, and twice the electromagnetic lengthening at each end, Δl [1]:

$$\Delta l = 0.412h\left(\frac{\varepsilon_{r_{eff}} + 0.3}{\varepsilon_{r_{eff}} - 0.258}\right)\frac{(W/h) + 0.264}{(W/h) + 0.8} \quad (3)$$

The resonant frequency for any TM_{mn} mode is then [1]:

$$f_r = \frac{c}{2\sqrt{\varepsilon_{r_{eff}}}}\left[\left(\frac{m}{(L + 2\Delta l)}\right)^2 + \left(\frac{n}{W}\right)^2\right]^{1/2} \quad (4)$$

Where c is the speed of light in free space, and m and n are integers representing the resonance modes of the length and width, respectively. It should be noted that these formulae are valid for very thin patch antennas, and were used to compare the resonant frequencies of the LiPo battery against a thin MPA of the same size.

In order to properly radiate fringing fields, so that the patch does not act simply as a capacitor, the ground plane should exist up to ≥ 5-10 substrate thicknesses from the edges of the patch. Another requirement in patch antenna design is that the substrate height should be less than 5% of the effective wavelength. These were all accounted for the experimental PCB design.

C. Proximity Coupled Feed

Proximity coupling uses a microstrip line located beneath the patch as a non-contact feed line. This is separated from the patch by a second substrate, as shown in Fig. 1.

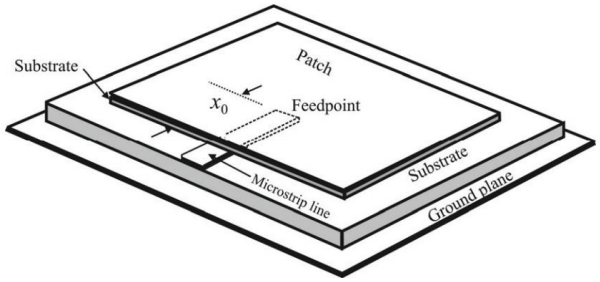

Fig. 1. Proximity coupled feed configuration of an MPA [1].

This technique raises the overall dielectric height, which increases the bandwidth of the MPA (up to a maximum of 13% in previous research [4]). However, the insulating layer of the LiPo battery used in this experiment was very thin, and therefore did not significantly increase bandwidth.

In order to match the input impedance of the patch to that of the feed line, the inset feed distance x_0 must be chosen so that the two are equal. This is discussed in detail in the next section. Another method is to use a matching stub along the feed line, although this can cause cross-polarisation, and is not preferable [5].

D. Impedance Matching

Indicative voltage and current distributions along the resonant length of a patch antenna are shown in Fig. 2, along with the resultant input impedance curve (Z_{in}). Z_{in} is a maximum at the edges of the patch (typically around 150Ω to 300Ω [1]), and goes to zero at its centre. A feedline with a characteristic impedance below the edge impedance of the patch can be matched to Z_{in} of the patch by selecting the feed point such that the two are equal. This is shown in Fig. 2 for a 50Ω feed line.

For a patch located above a microstrip feed line with an open circuit termination, the standing wave present on the feed line can be used to create an impedance match. The input impedance along such a standing wave, measured from the open circuit termination, is proportional to [8]:

$$Z_{in}^{OC} \propto \cot(\beta l) \quad (5)$$

Where β is the phase constant of the signal on the line, and l is the distance from the load impedance. The spatial period of this cotangent function is $0.5\lambda_{eff}$, which will be the separation between impedance matches along the feed line.

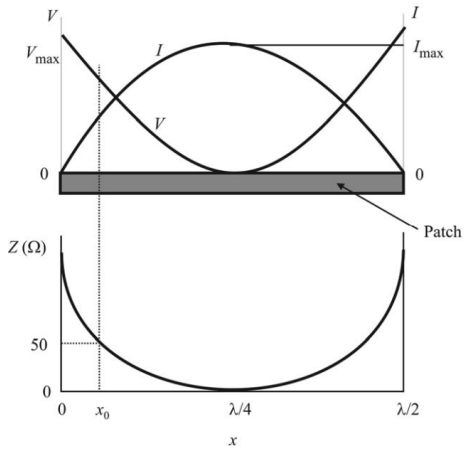

Fig. 2. Indicative voltage, current and impedance along the length of a half-wavelength patch. The feed point is located at x_0 to match the input impedance of the patch to a 50Ω feed line.

In reality, a patch (or battery) situated above the feed line would alter the fields (and input impedance) of the standing wave. This would change the exact location of the impedance match from what would be predicted from (5). Also, at the end of the feed line, fringing fields extend into free space, which has an effective permittivity lower than that of the feed line. This increases the effective wavelength, and so an impedance match to the patch due to these fringing fields would occur further than half an effective wavelength away from the last matching point along the feed line.

E. Lithium-Polymer Battery Design

LiPo batteries are composed of multiple conducting and insulating layers in a liquid electrolyte, all encased in aluminium film (as shown in Fig. 3) [9]. The entire battery is then encased in a plastic polymer (hence the term lithium polymer). The battery used in this experiment was housed in a thin polymer film.

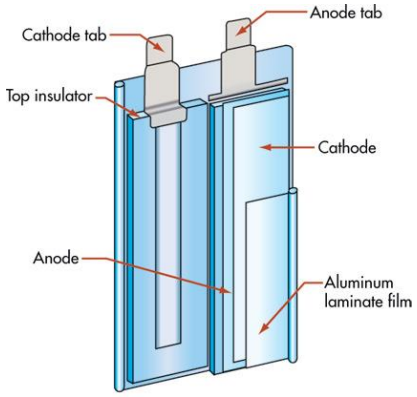

Fig. 3. Inner components of a LiPo battery cell. Figure produced by J. Vanzwol [9].

To drive a LiPo battery as a stable patch antenna equivalent, the relative permittivity of its components should remain relatively constant. Although this would be the case for a battery that is not charging and/or discharging, such transfers of charge could alter the radiating efficiency of the battery. Also, patch antenna design is based on the use of a single, thin conductive layer. Since patch antennas radiate via edge fringe fields, the multiple layers and aluminium casing of a LiPo battery could result in resonant frequencies and radiation patterns different to that of a normal patch antenna.

III. Experimental Method

The PCB in this experiment consisted of a 15cm microstrip feed line fabricated on a FR4 substrate with a sufficiently large copper ground plane (entire bottom layer). Soldered on one end of this feed line was a 50Ω SMA connector. The microstrip line was made to be 2.73mm wide so that it would also be 50Ω. This width was determined using an online module [10], for an FR4 substrate 1.6mm thick with a relative permittivity of 4.58. Since FR4 permittivity can vary with different resin to glass ratios, and is also frequency dependent [11], the nominal value provided by the Kingboard manufacturer was used. A via to the ground plane was also included on the board, away from the feed line, to allow for connection of the battery anode to ground. Fig. 4 shows the experimental setup with a grounding wire connected between the anode tab of the battery and the via to ground.

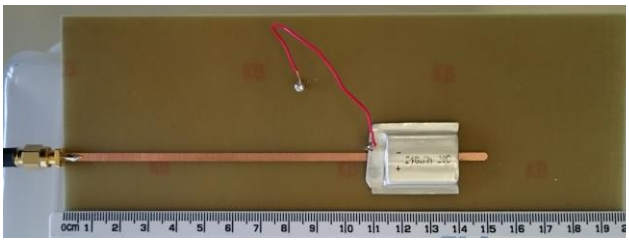

Fig. 4. Experimental setup for a grounded, tabs down (vertical) configuration. The microstrip feed line was centred along the width of the PCB (the bottom half is cut off in the above photo).

The VNA used to measure return loss was first calibrated using short, open and 50Ω terminations, before being used to measure the return loss of a LiPo battery placed on top of the feed line. The battery's position along the feed line was manually adjusted in minute increments to achieve strong resonances (RL < −20dB). The distance between the feeding edge of the PCB and the closest edge of the battery (excluding the tabs and polymer casing), was designated as *d*. This was recorded for each resonance, along with the minimum return loss. These measurements were made with and without a grounding wire, for multiple orientations of the battery (perpendicular to the feed line). These configurations were referred to in terms of the orientation of the battery tabs with respect to the SMA connector (looking towards the battery). The grounding wire was used to roughly emulate the battery's connection to ground in real circuits.

Sub-millimeter positional adjustments were required to achieve strong resonance (low return loss) in all cases. This limited the number of results obtained with the grounding wire, as its rigidity interfered with such fine adjustments. Return loss was also very sensitive to the angular orientation of the battery with respect to the feed line. This were accounted for as best as possible through careful alignments by eye.

Any objects (particularly conductive ones) in close proximity to the setup distorted the return loss plots on the VNA. This external interference was minimised by placing the PCB on a plastic box, in order to separate it from the conductive laboratory bench. All recorded measurements were taken with external objects (hands, body, ruler, etc.) well away from the LiPo battery.

The main sources of error in the experimental results were uncertainties in the feed line distance *d*, and angular orientation of the battery (not perfectly perpendicular). These uncertainties were both worsened when using the grounding wire.

A. AWR Simulations

AWR was used to simulate a single layer patch antenna equivalent to the experimental setup. A printed copper feed line was located on a FR4 substrate with a copper ground plane. Above this was a printed copper patch sandwiched between two layers of dielectric, having the ε_r of propylene film to simulate the polymer casing of the battery. The physical dimensions of the battery, polymer film and substrate were measured with a digital micrometer, and used to design the simulated elements. An SMA connector was also used in the simulation, from a standard component library.

Frequency sweeps were performed for the orientations of the battery used in the experiment, at incremental lengths along the feed line. Due to limited computational resources at the time of simulation, distances from the SMA connector were limited to 100mm (i.e. only matching by the standing wave, not fringing fields). The RL plots for resonances less than -20dB were recorded. A grounding wire was not included in any simulations. Comparisons between simulated and experimental results were therefore limited to non-grounded configurations.

IV. Results

Vertical and horizontal orientations refer to the longer dimension of the battery being aligned parallel and perpendicular to the feed line, respectively. 'Up' and 'down' (vertical configurations) refers to the tabs on the battery facing away from or towards the SMA connector, respectively. This is similar for 'left' and 'right' (horizontal configurations). 'Open' refers to no ground wire being used, and 'ground' refers to the use of one.

For both vertical and horizontal configurations, the resonant frequencies of a thin MPA, equal in size to the battery, were calculated using (4) for the fundamental TM_{10} mode. These frequencies were 2.89GHz and 3.71GHz, for vertical and horizontal orientations, respectively. For comparison, these are included in Fig. 6 and Fig. 7 as the fixed frequency dashed lines. Both TM_{20} (2nd order length resonance) and TM_{11} (1st order cross-polarisation for off-centre feeding) modes resonate at frequencies beyond the frequency range of the VNA used. This was true for both vertical and horizontal configurations.

A. Vertical Configurations

All simulated resonances occurred at 3.1GHz, with smaller return loss nulls (around -10dB at most) occurring at a variety

of different frequencies throughout simulation. These were due to different standing wave amplitudes at the receiver for each frequency, and were also observed in experimental return loss results.

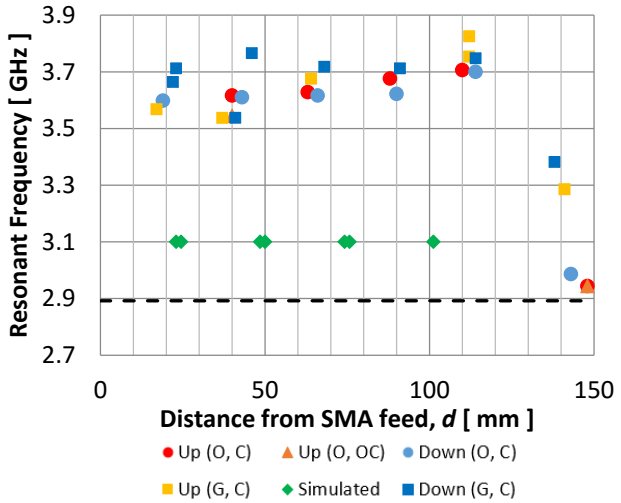

Fig. 6. Resonant frequencies for battery positions along the feed line for open and grounded vertical orientations.
O – Open, G – Grounded, C – Centred, OC – Off-Centre
Dotted line – Resonant frequency of an equal size, thin MPA

For each configuration, relative consistency in the resonant frequency along the feed line (d < 120mm) was also observed experimentally. The separation distance between consecutive resonances in this range was also fairly constant, averaging to around 21mm. This was approximately equal to $0.5\lambda_{eff}$ (within the uncertainty of distance measurements) for the mean f_r of around 3.7GHz. This verified the use of a standing wave to achieve impedance matching, where such a match would occur every $0.5\lambda_{eff}$.

For resonances in the range d > 140mm, the majority of the battery extended beyond the feed line. Thus, impedance matches for these distances were due to the fringing fields at the feed line termination. This increased the separation distance from the previous resonance, due to the lower λ_{eff} for the feed line fringing fields (outlined in section II. *D*). Also, f_r for all configurations was decreased, likely due to the diverging fields of the feed line at its termination. Another important factor would have been the conducting tabs of the battery, which possibly increased the effective length and reduced f_r.

This change in f_r was not as significant for when the battery anode was grounded. Also for the grounded configurations, there were instances of distinct resonances closely spaced along the feed line (not near the termination). Both of these effects were probably the result of both the variability in battery orientation due to the grounding wire, as well as alterations in the current distribution within the battery due to the ground connection.

Without a grounding wire, both the simulated and theoretical resonant frequencies were significantly lower than the experimental results along the feed line. Most likely this was due to the physical differences between a planar patch and the more complicated, multi-layer LiPo battery. In particular, the different interactions of each geometry with a standing wave existing along a proximity feed line.

B. Horizontal Configurations

Results for horizontal configurations were much less consistent between different configurations than for the vertical configurations. In this case, while with the majority of simulated resonances occurred at 3.9GHz, three simulated results were within the range of experimental f_r values.

For experimental resonances near 3GHz, separations between resonances were close to the corresponding $0.5\lambda_{eff}$ (24.5cm). This again verified the use of a standing wave to achieve impedance matching.

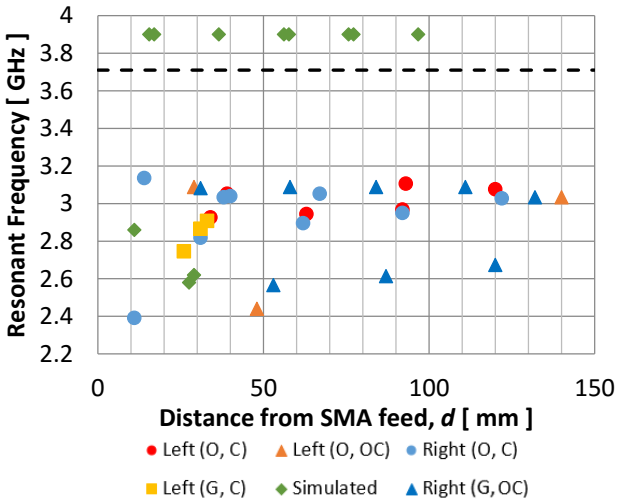

Fig. 7. Resonant frequencies for battery positions along the feed line for open and grounded horizontal orientations.
O – Open, G – Grounded, C – Centred, OC – Off-Centre
Dotted line – Resonant frequency of an equal size, thin MPA

The lower resonant frequencies for horizontal configurations were due to the shorter resonant dimension of the battery, but also the fact the W/L > 1. This increased $\varepsilon_{r_{eff}}$, which further reduced f_r.

Resonances due to feed line fringing fields (near termination) were not located further from the SMA, as they were for vertical configurations. Also, there was no shift in f_r for these fringing field impedance matches. This may have been due to the battery tabs not being oriented along the resonant length of the battery.

For the off-centre feeding, two different resonant frequencies were clearly present. Since the f_r values of higher order TM modes were outside the S band, this must have been the result of the LiPo battery design. Its inner components may behave differently when driven along the width of the battery. Also, the electrode tabs may have modified the width of the battery for n mode resonances.

The minimum return loss in the entire experiments was measured for an open right configuration, at -70dB. However, most return losses were between -35 and -50dB.

C. Impedance Bandwidths

Table I lists the averaged experimental impedance bandwidths for each configuration, excluding anomalously high bandwidths not associated with high resonance. Across all configurations, bandwidths ranged between 1.76% and 3.53%.

Without the use of a grounding wire, vertical orientations had higher bandwidths than horizontal orientations. This

would have been due almost entirely to the different *L* and *W* dimensions for each orientation.

TABLE I
AVERAGE IMPEDANCE BANDWIDTHS FOR DIFFERENT CONFIGURATIONS

	Tabs Up	Tabs Down	Tabs Left	Tabs Right
Open	3.391	3.025	2.571	2.864
Ground	3.528	2.867	1.759*	^

*Only three measurements were taken to calculate this average
^No measurements were made for this configuration
Impedance bandwidths were measured for $RL < -10\text{dB}$

The direction of the battery's electrode tabs appeared to alter the bandwidth for all 'open' configurations, as well as the vertical grounded setup. It should be noted that this may have also been due to the effects of internal battery components. The largest difference in bandwidth for tab orientation was between the two vertical grounded configurations.

The small number of results obtained for horizontal grounded configurations precluded effective comparisons regarding a grounding wire's effect on impedance bandwidth.

V. CONCLUSIONS

A rectangular LiPo battery was driven as a modified patch antenna at resonant S band frequencies using proximity coupling. Low return losses between -35 and -50dB were consistently achieved, indicating that such a battery can be efficiently resonated as a patch antenna equivalent. However, as with other patch antennas, the measured impedance bandwidths were relatively small. Although multiple frequency channels were usable, these appear to be difficult to predict based only on the dimensions of a battery.

Also, due to the sensitivity of the return loss to the position of the battery along the feed line, a LiPo battery driven as a patch antenna would need to be fixed securely in place to ensure a stable radiated frequency. This may require additional components in some electronic devices.

Radiation patterns and pattern bandwidths of the LiPo battery should be measured to determine the full suitability of LiPo batteries as patch antenna equivalents. Testing should also be undertaken for a battery being charged and discharged within a practical circuit. Additional grounding configurations could also be investigated as part of future research.

ACKNOWLEDGMENT

The author would like to acknowledge the partnership of J. Tailby in conducting this experiment, as well as the knowledge and guidance provided by D. Thiel, H. Espinosa and F.Majeed.

REFERENCES

[1] R. Poisel, *Antenna Systems and Electronic Warfare Applications*. Norwood, MA: Artech House, 2012.

[2] C.-M. Su, K.-L. Wong, C.-L. Tang, and S.-H. Yeh, "EMC internal patch antenna for UMTS operation in a mobile device," *Antennas and Propagation, IEEE Transactions on*, vol. 53, pp. 3836-3839, 2005.

[3] D. M. Pozar, "Microstrip antennas," *Proceedings of the IEEE*, vol. 80, pp. 79-91, 1992.

[4] D. M. Pozar and B. Kaufman, "Increasing the bandwidth of a microstrip antenna by proximity coupling," *Electronics Letters*, vol. 23, pp. 368-369, 1987.

[5] H. Rmili, J.-L. Miane, H. Zangar, and T. Olinga, "Design of microstrip-fed proximity-coupled conducting-polymer patch antenna," *Microwave and Optical Technology Letters*, vol. 48, pp. 655-660, 2006.

[6] J. R. Ojha and M. Peters. (2010). *Patch Antennas and Microstrip Lines*. InTech: Germany

[7] C. A. Balanis, *Antenna Theory: Analysis and Design*, 3 ed. Hoboken, New Jersey: Wiley, 2012.

[8] F. T. Ulaby, E. Michielssen, and U. Ravaioli, *Fundamentals of Applied Electromagnetics*, 6 ed. Upper Saddle River, NJ: Pearson, 2010.

[9] J. Vanzwol, "LiPo cell construction,", 2011.

[10] F. T. Ulaby, E. Michielssen, and U. Ravaioli, *Lossless microstrip line*, 2015 [Online]. Available: http://em.eecs.umich.edu/ch2/mod3. [Accessed: 20 Aug 2015]

[11] D. Ionescu and I. B. Ciobanu, "Study in Microwave Range of some HF Board Materials for Lead-Free Technologies," *Romanian Reports in Physics*, vol. 61, pp. 676-688, 2009.